

Restricted Diffusion in the Regime of the Order-to-Disorder Transition in Diblock Copolymers: A Field Gradient NMR Study

G. Fleischer

Fachbereich Physik, Universität Leipzig, Leipzig, Germany

F. Fajara

Institut für Physikalische Chemie, Universität Mainz, Mainz, Germany

B. Stühn*

Fakultät für Physik, Universität Freiburg, Freiburg, Germany

Received October 13, 1992; Revised Manuscript Received January 21, 1993

ABSTRACT: The self-diffusion of diblock copolymers of polystyrene/*cis*-1,4-isoprene and polyisoprene homopolymers is studied using field gradient nuclear magnetic resonance. The block copolymers are shown to go through their order-to-disorder transition (ODT) at experimentally accessible temperatures. Their phase state is determined using small-angle X-ray scattering. Diffusion in the ordered, lamellar phase is found to be spatially restricted. Fast motion is possible along the lamellae and within a grain. The crossing over the enthalpic barriers between styrene and isoprene domains takes place on a much longer time scale. The ODT does not lead to an abrupt crossover to unrestricted diffusion. Local order remains even above the ODT, and the barriers disappear only gradually.

I. Introduction

The self-diffusion of macromolecules in their melt is a complex phenomenon which has attracted considerable attention in recent years. Over distances that are short compared to the molecules' radius of gyration it involves the large number of internal degrees of freedom. The main characteristics of diffusion in this regime are comprised by the Rouse model which leads to a nonlinear dependence of the mean-squared displacement of a segment on diffusion time. Only for long times, corresponding to displacements larger than the radius of gyration, is normal diffusion recovered.

In the present study we have investigated the self-diffusion of polystyrene/*cis*-1,4-isoprene diblock copolymers. Due to the relatively short length of the polymers, chain entanglements do not play a role. However, the self-diffusion is modified by the introduction of a specific order in the liquid: at low temperatures the effective repulsion between the blocks of the molecule leads to a phase transition, the microphase-separation transition (MST). It effectively stretches the molecule in order to minimize the number of contacts between both blocks and ends in a periodic arrangement of styrene- and isoprene-rich domains. The typical lengths thus introduced into the system are the periodicity and the domain size of the structure.

It is obvious that self-diffusion will be influenced by the existence of this type of order in the liquid. The strong enthalpic barrier between styrene and isoprene domains will suppress diffusion across the domain boundaries. Recent experiments using forced Rayleigh scattering showed indeed an unusual diffusion of dye-labeled molecules in the lamellar phase of a diblock copolymer which was interpreted as anisotropic diffusion along the lamellae.¹

The internal diffusion in the disordered state has been shown to be only weakly influenced by the interaction between styrene and isoprene segments.² It is well described in a Rouse model including the interaction in a mean-field theory.

The polymers used in our study are nearly symmetric diblocks which show the phenomenon of MST at experimentally accessible temperatures. It is thus possible to investigate the self-diffusion of the macromolecule in both the ordered and the disordered state. The experimental method used is field gradient NMR. It essentially monitors the self-diffusion of the polyisoprene block over distances larger than the radius of gyration. We will briefly describe this experimental technique in the following section.

In order to relate the diffusion experiment to structural properties of the system, we will then characterize the diblock copolymers using results from small-angle X-ray scattering (SAXS). These measurements define the relevant lengths of the system and provide the temperature of the MST. We will show that field gradient NMR experiments are perfectly suited for the investigation of diffusion on intermediate length scales. Their interpretation is possible in the concept of the incoherent dynamic structure factor which, on shorter scale, is measured using neutron scattering. The order created by the MST in the melt of a diblock copolymer leads to spatial confinement of the molecule.

II. Experimental Method: Field Gradient NMR

The aim of this section is to provide the basic formalism which is necessary to extract the dynamic properties of the diffusing molecule from the experiment. We will emphasize the conceptual similarity between field gradient NMR and quasielastic incoherent neutron scattering which has successfully been used to study polymer dynamics in the past. A more detailed description of the field gradient NMR method may be found elsewhere.³

The basis of the technique is a stimulated echo measurement using the proton spin as a probe. Consider a 3-pulse sequence as depicted in Figure 1. In the case of $t \gg \tau$ the echo amplitude $\Psi(\tau, t)$ can be written as a single-particle correlation function

$$\Psi(\tau, t) \propto \underbrace{\langle \cos[\Phi(t=0)] \cos[\Phi(t)] \rangle}_{S(\tau, t)} e^{(-\tau/T_2)} e^{(-t/T_1)} \quad (1)$$

with the spin-spin relaxation time T_2 and the spin-lattice relaxation time T_1 . The phases $\Phi(t=0)$ and $\Phi(t)$ are acquired by the tagged particles in the "dephasing" and the "rephasing"

* To whom correspondence should be addressed.

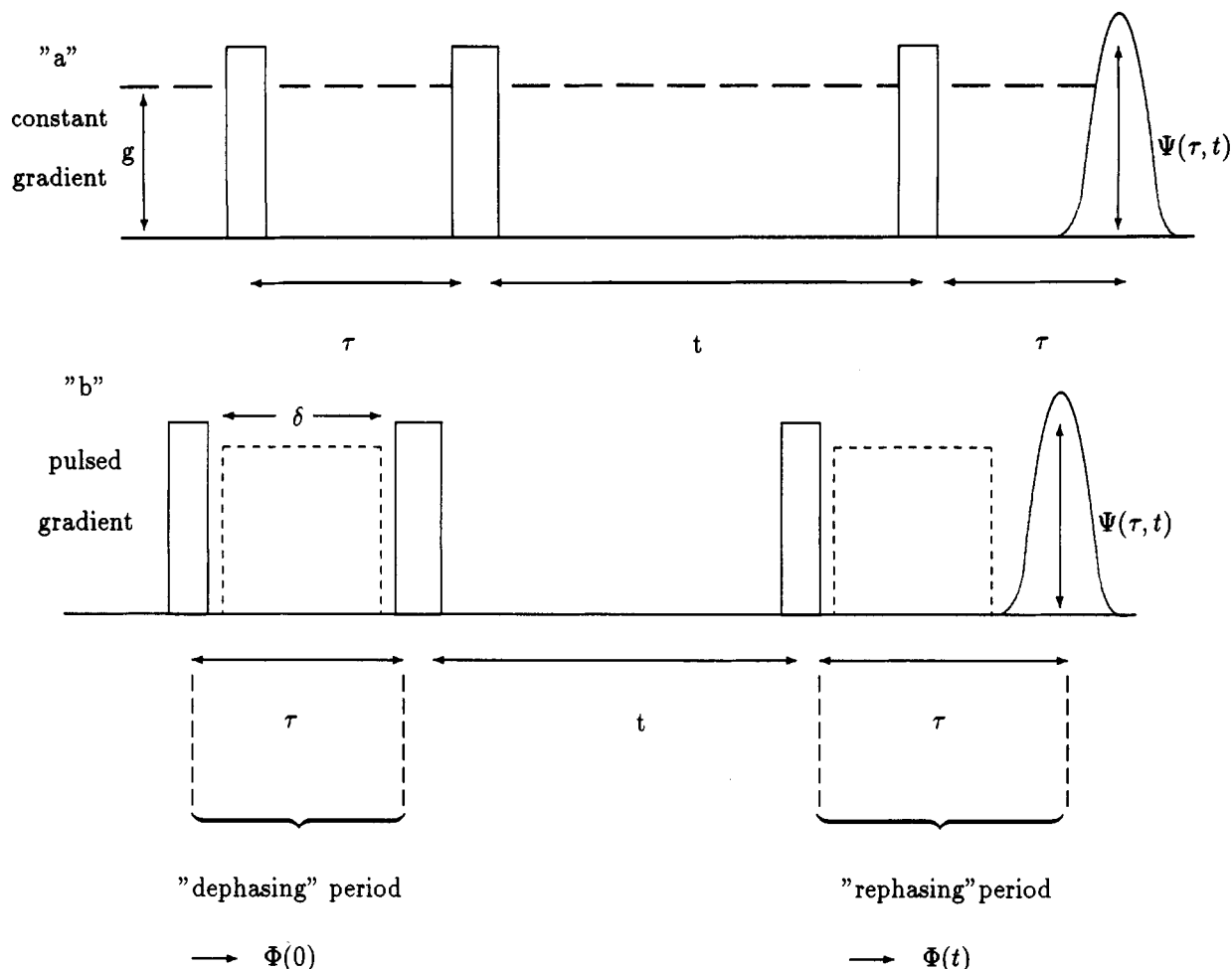


Figure 1. Schematic view of the pulse sequence in a spin-echo NMR experiment. Each radio-frequency pulse rotates the proton spin by 90° . In a the field gradient of magnitude g is permanently switched on, in b it is pulsed with duration δ . At time $t + 2\tau$ the spin echo occurs with amplitude $\Psi(\tau, t)$.

period, respectively. The broken brackets $\langle \rangle$ denote the ensemble average. In an NMR experiment a phase Φ is always given as the product of the instantaneous Larmor frequency $\omega_{\text{NMR}}(t) = \gamma B(t)$ and the precession time τ in the transversal plane

$$\Phi(t) = \omega_{\text{NMR}}(t) \tau = \gamma B(t) \tau \quad (2)$$

with γ denoting the gyromagnetic ratio and $B(t)$ the amplitude of the instantaneous local magnetic field. The direction of B defines the quantization axis.

If the field B varies in the volume of the sample with a time-independent gradient g , i.e.

$$B(t) = g \cdot r(t) \quad (3)$$

we may define a generalized scattering vector

$$q = \gamma g \tau \quad (4)$$

Using eqs 2–4 in eq 1, we obtain

$$\begin{aligned} S(\tau, t) &\rightarrow S(q, t) = \langle \cos[q \cdot r(0)] \cos[q \cdot r(t)] \rangle \\ &= \langle \cos[q \cdot (r(0) - r(t))] \rangle \\ &= \int d^3 r_0 \int d^3 r p(r_0) P(r, r_0, t) \times \\ &\quad \cos[q \cdot (r - r_0)] \quad (5) \end{aligned}$$

$p(r_0)$ is the probability of finding a spin at the position r_0 at time 0, and $P(r, r_0, t)$ is the conditional probability for the spin to move over the distance $r - r_0$ during the time interval t . $S(q, t)$ is therefore the Fourier transform of the autocorrelation function for the proton position. It may be identified with the normalized intermediate scattering function $S(q, t)$ observed in incoherent neutron scattering.^{4,5} The generalized "scattering vector" q defined in eq 4 can be changed either by variation of the gradient g or by variation of the dephasing time τ . In the following we restrict attention to isotropic samples and therefore only the length $q = |q|$ is important.

Typical values of q achieved in our experiments are realized with a gradient $g = 45 \text{ T/m}$ and $\tau = 10^{-3} \text{ s}$ which results in $q = 1.2 \times 10^{-2} \text{ nm}^{-1}$. This is about 1–2 orders of magnitude smaller than the smallest q obtained in quasielastic neutron scattering. Field gradient NMR is therefore ideally suited to extend the range of observation to larger distances.

An important example for the application of eq 5 is the free diffusion of a particle in an isotropic medium. In that case we have a Gaussian probability $P(r, r_0, t)$ and $p(r_0) = \text{const}$. Equation 5 then yields

$$S(q, t) = e^{-q^2 D t} \quad (6)$$

with D the self-diffusion coefficient. The more complicated situation of diffusion in a restricted volume is relevant for the discussion of our measurements. We will return to this topic in section IV.

Two different techniques were used in the experiments. Their mode of operation is schematically depicted in Figure 1. Method a uses a permanent field gradient g . The experiments are performed in the stray field of a cryomagnet.⁶ q is given by eq 4. Method b uses field gradient pulses of strength g and duration $\delta < \tau$. In this case dephasing occurs only while the gradient is switched on. For q one thus has a slightly modified expression:

$$q = \gamma g \delta \quad (4a)$$

Both methods are complementary. The permanent gradient method a does not allow for an easy change of the gradient strength. A change of q can only be achieved by a variation of the dephasing time τ which in turn also changes one of the relaxation prefactors (see eq 1). This disadvantage is compensated by the possibility of extending the experiments to very small values of τ , the only limitation being the spectrometer "dead time" of a few microseconds.

In the pulsed gradient method b, on the other hand, q can be changed via the gradient amplitude g and the pulse duration δ .

Table I
Characterization of the Polymers Used

sample	f , vol fraction of PS	M_w	M_w/M_n	T_g/K
Block Copolymers				
B1	0.44	15 700	1.04	390
B2	0.50	10 500	1.04	336
Polyisoprene Homopolymers				
H2		8 200		
H3		15 500		

This has no influence on the relaxation prefactors. However, switching the gradient on and off does not allow us to reduce δ below, say, 10^{-3} s. Large q values require strong magnetic field gradients and are limited by thermal and mechanical problems with the large currents in the field gradient coil.³

It is seen from eq 1 that the longest accessible diffusion time t is determined by the spin-lattice relaxation time T_1 . In favorable cases T_1 is on the order of seconds. In general, t may be varied between 10^{-3} s up to T_1 . Another limitation is imposed by the spin-spin relaxation time T_2 , which sets the upper limit of the accessible q -range.

In our present case the proton NMR signal stems from both diblock components. Since T_2 is very short for polystyrene, the experiment is essentially sensitive to the diffusion of the polyisoprene block alone.

III. Microphase Separation and Order in the Diblock Copolymers

Diblock copolymers of polystyrene and polyisoprene are mostly obtained in their microphase-separated state: depending on the volume fraction f of polystyrene, they form domains of spherical, cylindrical, or lamellar symmetry. The reason for the existence of this type of order lies in the repulsive interaction between both blocks. In a lattice model of the disordered state its contribution to the local free energy per lattice point G_{loc} is described in terms of the Flory-Huggins parameter χ

$$\chi = -\frac{1}{2k_B T} \frac{\partial^2 G_{loc}}{\partial f^2} \quad (7)$$

χ is found to display the simple temperature dependence $\chi = A + B/T^{7.8}$ and the parameters A and B appear to depend on the composition f .⁹ Lowering the temperature increases the weight of the interaction described in G_{loc} to the free energy. In a mean-field theory, the random-phase approximation (RPA),¹⁰ one predicts a phase transition to occur which for $f = 1/2$ is of second order. The ordered state consists of a lamellar structure of polystyrene and polyisoprene domains. It was found, however, that the contribution of concentration fluctuations to the free energy may not be neglected.¹¹ This leads to a modified picture of the MST rendering it a fluctuation-induced phase transition of weakly first order.

The diblock copolymers used in this study are of nearly symmetric composition ($f \approx 1/2$) and narrow molecular weight distribution. Their characterization is given in Table I. In the following we summarize data from small-angle X-ray scattering (SAXS) obtained from B1¹² and B2¹³ in order to describe the structure of concentration fluctuations and the degree of order in both systems.

The intensity measured at a scattering vector q in a SAXS experiment is directly proportional to the correlation of concentration fluctuations $\delta\phi$ in the system

$$I(q) = K \langle \delta\phi_{-q} \delta\phi_q \rangle \quad (8)$$

K is a contrast factor given in terms of the electron densities of polystyrene and polyisoprene.

An example of a scattering profile obtained in the disordered state of B1 is given in Figure 2. The broad

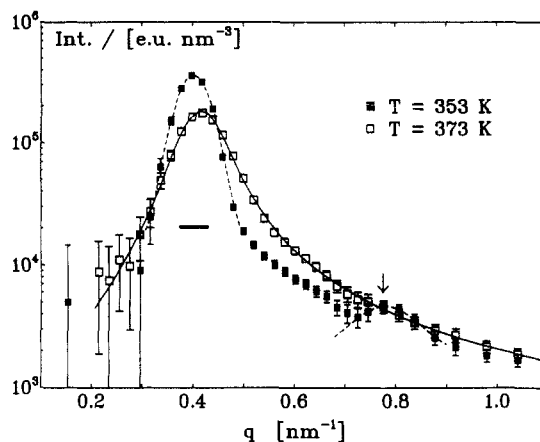


Figure 2. SAXS profiles of the diblock copolymer sample B1 in the disordered ($T = 373$ K) and in the ordered state ($T = 353$ K). The horizontal bar is an estimate of the angular resolution. The drawn line corresponds to a fit with RPA theory; the broken lines show the positions of the Bragg peaks from the ordered structure. The arrow marks the position of the second-order peak.

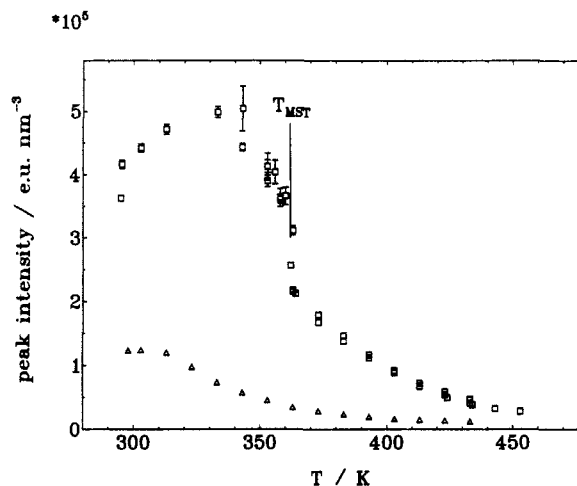


Figure 3. Temperature dependence of the SAXS peak intensity $I(q^*)$ for the block copolymers B1 (\square) and B2 (Δ). The MST is clearly seen as a discontinuous jump in peak intensity for B1, whereas for sample B2 the glass transition of the polystyrene domain prevents the formation of long-range order.

peak visible in the SAXS intensity is caused by the block structure of the molecule and by the repulsive interaction between its blocks. The detailed structure factor may be calculated on the basis of RPA theory^{9,10} and gives a good description of the data. The radius of gyration R_g of the diblock in the disordered state is determined to be 4.1 nm. With lowering T to the MST it increases by 10%.¹² The good fit of the RPA structure factor for $0.8 \leq qR_g \leq 4.5$ supports the picture of the disordered state as consisting of randomly interpenetrating, Gaussian coils.

The transition to the ordered structure is also shown in Figure 2. It is observed in the transformation of the broad peak into a narrow, intense Bragg peak at $q^* = 0.38 \text{ nm}^{-1}$. A second order appears at $2q^*$. From peak position and width the structure is determined to consist of lamellae of thickness $d = 16.2 (\pm 0.1) \text{ nm}$ and a domain size of 310 nm.¹²

For polymer B2 the formation of long-range order is not observed. It is stopped by the glass transition of the polystyrene domains.¹³ In the case of B1 the glass transition occurs 40 K below the MST.

Figure 3 shows the temperature dependence of the peak intensity $I(q^*)$. In the case of sample B1 the transition temperature is clearly defined at the abrupt increase of

Table II
Segmental Friction Coefficients and Activation Energies

sample	\bar{N}^a	ζ_0^b (kg s ⁻¹)	E_A^c (kJ mol ⁻¹)
B1	196	1.45×10^{-10}	80
B2	127	1.80×10^{-10}	60
H2	120	9.50×10^{-12}	30
H3	230	1.80×10^{-11}	30

^a Number of monomers. ^b At $T = 413$ K. ^c Between 390 and 413 K.

the intensity: $T_{\text{MST}} = 362$ K. Such a sudden increase is not found for B2.

The temperature variation of I at high T is described by a spinodal temperature T_s (see Table I) such that

$$\frac{1}{I(q^*)} \propto \frac{1}{T_s} - \frac{1}{T} \quad (9)$$

Lowering T enhances concentration fluctuations in particular at a wavelength $\lambda^* = 2\pi/q^*$ and thus leads to an increase of the intensity $I(q^*)$. At $T = T_s$ this intensity should diverge.

However, about 30 K above T_{MST} the measured intensity is lower than predicted by eq 9.⁹ This has led to the conclusion that long-living concentration fluctuations are present in the system which violate the mean-field assumption of the RPA. A separation of polyisoprene and polystyrene on local scale exists without long-range correlation.

The decrease of $I(q^*)$ below 340 K for B1 (see Figure 3) is caused by a loss of contrast between the polystyrene and polyisoprene domains. Below 340 K the polystyrene domains are in their glassy state and their density therefore remains essentially constant with further lowering of the temperature. The polyisoprene density, however, further increases and consequently the density difference between both domains becomes smaller.

In summary the diblock copolymers are shown to exist in a disordered state at high temperatures. With lowering of the temperature polymer B1 spontaneously forms a lamellar structure at T_{MST} , whereas B2 remains in a locally ordered state due to the glass transition of the polystyrene domain. The field gradient NMR experiments were performed in the temperature range from 320 to 420 K. They extend from the ordered state into the fluctuation controlled regime.

IV. Results and Discussion of the Field Gradient NMR Measurements

This series of experiments involves both diblock copolymers B1 and B2 as well as two homopolymers of polyisoprene H2 and H3.

The homopolymers are of molecular weights comparable to the isoprene blocks and the total copolymer, respectively (see Table I). The self-diffusion measurement on homopolymers using field gradient techniques has been described earlier. The measurements are in agreement with eq 6; the self-diffusion coefficients agree with earlier measurements.¹⁴ In particular there is no influence from entanglements. The results are shown in Figure 8. The corresponding friction coefficients and activation energies are given in Table II. They are in agreement with dielectric normal-mode experiments on the same polymers.¹⁵

Completely different results were obtained from the block copolymers. Figure 4 displays the echo amplitude Ψ for sample B1 using the constant gradient method of Figure 1a. The data refer to an effective wavevector $q = 3.6 \times 10^{-3} \text{ nm}^{-1}$ at $T = 329$ K, i.e., in the ordered state. The

$\times 10^3$

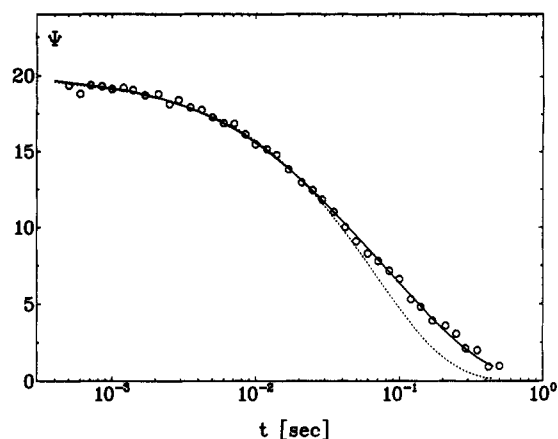


Figure 4. Spin-echo signal of sample B1 as measured with field gradient NMR at an effective scattering vector $q = 3.6 \times 10^{-3} \text{ nm}^{-1}$ and $T = 329$ K. The drawn line is a fit of eq 13; the dotted line corresponds to a freely diffusing particle (see text).

decay of the echo signal caused by T_1 has been determined in a measurement at very small τ (corresponding to $q \rightarrow 0$).

The figure shows a fast decay of Ψ at short times which slows down at intermediate times. The remaining decay in the echo signal is due to the spin-lattice relaxation time T_1 . This is made evident in the figure by comparing the data with an echo signal referring to a single-exponential decay as obtained from inserting eq 6 into eq 1. This model of an unrestrictedly diffusing particle fits the data over nearly 2 decades in time. At long times, however, the data deviate clearly from this model. Using eq 1 to reduce Ψ to the scattering function $S(q, t)$, one finds that $S(q, t)$ attains a nearly constant level at long times. The existence of this level is clear evidence for the presence of spatial constraints on the diffusion of the polymer.

In an incoherent neutron scattering experiment the constant fraction of the intermediate scattering function $S(q, t)$ is denoted the elastic incoherent scattering factor (EISF):⁴

$$\text{EISF} = \lim_{t \rightarrow \infty} S(q, t) / S(q, 0)$$

Its q dependence may be used to measure the size of the effective cage in which the particle is allowed to diffuse.

For a discussion of our results we adopt the following model. We assume the molecule to diffuse parallel to the lamella. Otherwise the polyisoprene block would have to cross the polystyrene domain. In these two dimensions the diffusion is restricted to the extension of the lamella. It is stopped at grain boundaries. Effectively the particle is therefore confined in a cylindrical box of radius R , the grain size, and height $h \approx d/2$. From the SAXS results (section III) it is concluded that $h \ll R$.

The diffusion of a particle in a closed volume V is in general described by solving the diffusion equation for the correlation function $P(\mathbf{r}, \mathbf{r}_0, t)$ (see eq 4) for the boundary condition $P \equiv 0$ on the surface of V .⁴ For the present case of a disk-shaped cylinder the problem is solved by assuming the diffusion along the cylinder axis and perpendicular to be uncorrelated.¹⁶ For small wave vector q one arrives at

$$S(\mathbf{q}, t) = 1 - \frac{q_R^2 R^2}{4} - \frac{q_z^2 h^2}{8} + Q(\mathbf{q}, t) \quad (10)$$

$Q(\mathbf{q}, t)$ is the time-dependent part of S and is in general a complex superposition of exponentials.¹⁶ q_z and q_R denote the components of the wavevector along the cylinder axis and perpendicular to it. The sample in our

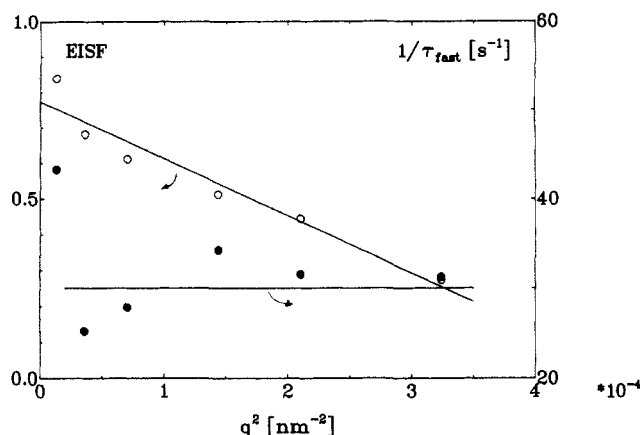


Figure 5. Elastic incoherent structure factor (left scale) and the time τ_{fast} (see eq 13) for sample B1 in the ordered state ($T = 329$ K).

experiment is macroscopically isotropic. Equation 10 therefore has to be averaged over all directions of \mathbf{q} . Because of $h \ll R$ we obtain

$$S(q, t) = 1 - \frac{q^2 R^2}{3} + \bar{Q}(q, t) \quad (11)$$

The detailed form of eq 11 depends on the geometry of the confinement. For the case of a sphere of radius R the factor $q^2 R^2/3$ has to be replaced by $2q^2 r^2/5$.

In view of the limited spectral range of the experiment we approximate the orientational average $\bar{Q}(q, t)$ as

$$\bar{Q}(q, t) \approx Q_0 e^{-t/\tau_{\text{fast}}(q)} \quad (12)$$

$D_{\text{fast}} = (\tau_{\text{fast}} q^2)^{-1}$ is to be considered an effective diffusion coefficient for the block copolymer. It controls the time dependence of its mean-squared displacement within the box.

At very long times the plateau in $S(q, t)$ caused by the spatial restriction of diffusion is seen to decay itself. The cage confining the polymer is of finite lifetime and allows a further slow diffusion of the molecule. We take these effects into account in a model equation for $S(q, t)$:

$$S(q, t) = [\beta(q) + Q_0 e^{-t/\tau_{\text{fast}}(q)}] e^{-D_{\text{slow}} q^2 t} \quad (13)$$

Equation 13 together with eq 1 is used to analyze the spin-echo NMR data, and Figure 4 demonstrates the excellent quality of the fits thus obtained for the example of sample B1 in its ordered state ($T = 329$ K). In the case of a scattering experiment resolving only the fast dynamics, one would identify $\beta(q)/(\beta(q) + Q_0)$ with the EISF.

It is then possible to investigate the dependence of the EISF on q in order to characterize the size of the cage. Figure 5 shows the results of measurements on the same sample for various values of the wavevector q . The EISF is seen to be in good agreement with eq 11. The straight line corresponds to a radius $R = 70$ nm. Although the condition $qR_g \ll 1$ is well fulfilled by the data in Figure 5, the intercept at $q = 0$ is not 1. The origin of this deviation from the expectation of our model may be fast-diffusing impurities in the polymer (e.g., traces of solvent). They are known to enter the echo signal quite strongly because of their long nuclear magnetic relaxation times.¹⁷

In the same figure we show the result for $\tau_{\text{fast}}(q)$. At low q τ_{fast} turns out to be nearly independent of the wavevector as is to be expected in the case of spatially confined diffusion.⁴

The cage size R is nearly independent of temperature up to 397 K; i.e., spatial restrictions extend over the same range in the ordered state of the diblock as in the fluctuation controlled, disordered regime.

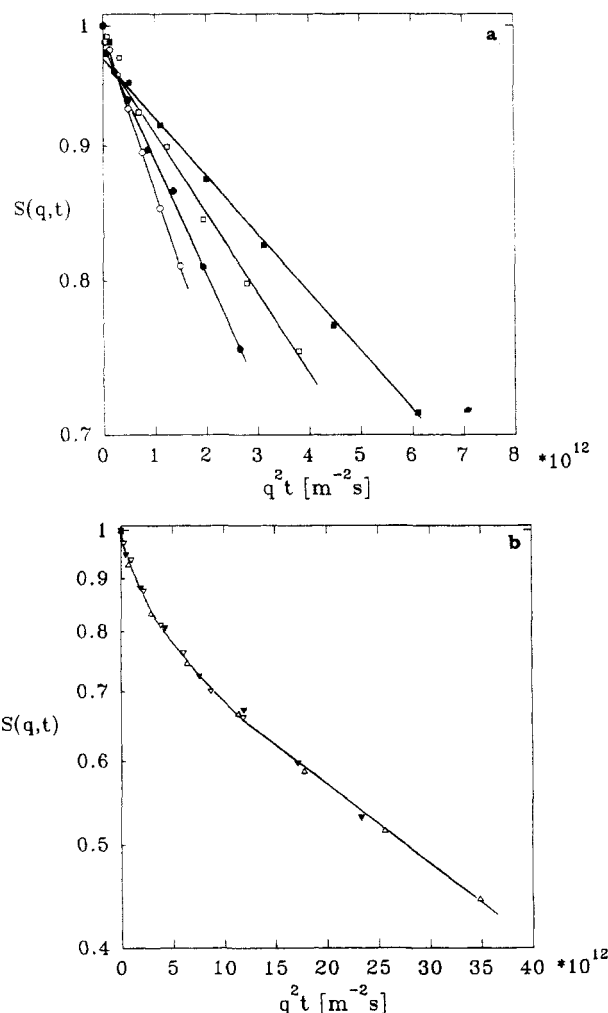


Figure 6. Semilogarithmic plot of $S(q, t)$ (sample B1) measured with the pulsed field gradient NMR at $T = 373$ K for (a) $t = 13$ ms (\circ), $t = 23$ ms (\bullet), $t = 33$ ms (\square), and $t = 53$ ms (\blacksquare) and (b) $t = 103$ ms (∇), $t = 203$ ms (\blacktriangledown), and $t = 303$ ms (\triangle).

The long-time diffusion coefficient D_{slow} is determined in this measurement to be $D_{\text{slow}} = 0.13 (\pm 0.02) \times 10^{-13} \text{ m}^2 \text{ s}^{-1}$. Its temperature dependence is given in Figure 8.

The pulsed field gradient experiment *b* (see Figure 1b) is a more direct access to the diffusion coefficient as it measures, at a constant time t , the mean-squared displacement $\langle r^2 \rangle_t$. One may thus define an apparent diffusion coefficient

$$D_{\text{app}} = \langle r^2 \rangle_t / 6t \quad (14)$$

with the limits

$$D_{\text{app}} \rightarrow D_{\text{slow}} \quad \text{for } t \rightarrow \infty$$

$$D_{\text{app}} \rightarrow D_{\text{fast}} \quad \text{for } t \rightarrow 0$$

The range of effective q vectors is smaller in this experiment and extends up to 10^{-2} nm^{-1} . Parts a and b of Figure 6 show the results for sample B1 at $T = 373$ K. The diffusion times range from 13 to 53 ms and from 103 to 503 ms, respectively. As was mentioned before there is no T_1 relaxation involved in this experiment. We observe an apparent self-diffusion coefficient decreasing with time. It is of the same order as that determined from the short-time behavior of $S(q, t)$ in Figure 5. The decrease of the apparent diffusion coefficient is a clear indication for restricted diffusion.³ For times $t > 100$ ms the diffusion process becomes stationary.

One thus derives two diffusion coefficients corresponding to the limits given in eq 14. They must be attributed

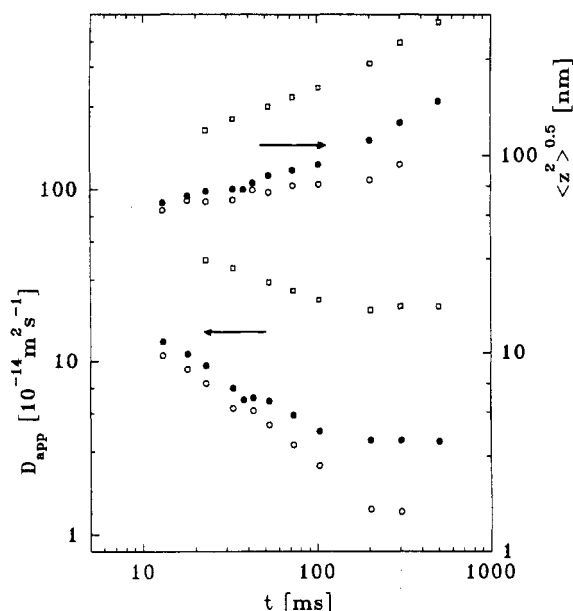


Figure 7. Apparent diffusion coefficient (see eq 14) and the mean-squared displacement determined with pulsed field gradient NMR for sample B1 at $T = 363$ K (○), $T = 388$ K (●), and $T = 413$ K (□).

to diffusion of the molecule within one domain (D_{fast}) and to a crossing of the domain boundaries with a much slower diffusion constant D_{slow} . Within the cage at $D_{\text{fast}} = 10^{-13} \text{ m}^2 \text{ s}^{-1}$ the molecule explores a mean-squared displacement of about 70 nm in 0.07 s. Referring back to Figure 4, it is seen that the deviation from unrestricted diffusion indeed becomes evident at this time.

Figure 7 shows the results for D_{app} as well as $\langle r^2 \rangle_t$ for three temperatures at the MST and in the fluctuation controlled regime. Immediately at the temperature of the phase transition the slow and the fast diffusion differ by an order of magnitude. At this stage the local constraints for the diffusion of the molecule are clearly active and result in a strong time dependence of the apparent diffusion coefficient up to mean-squared displacements of $\langle r^2 \rangle^{1/2} \approx 70$ nm.

Increasing the temperature leads to strong acceleration of diffusion at long times. About 50 K above T_{MST} the difference between D_{slow} and D_{fast} is only a factor of 2. The gradual disappearance of the cage does not occur through an enlargement of its scale but rather by an assimilation of diffusion within the cage and across its boundaries. The mixing of polystyrene and polyisoprene lowers the barrier for diffusion out of the cage.

Even in the mixed state at high temperatures the block copolymer diffuses much slower than a homopolymer of polyisoprene of a molecular weight corresponding to the block (H2) or the total molecular weight of the copolymer (see Figure 7) due to the low contribution of free volume by the polystyrene block.

The measurements on the shorter diblock copolymer B2 gave very similar results. They differ mainly in their temperature dependence as is shown in Figure 8. Whereas the long-time diffusion coefficient for B1 levels off for low temperatures, there is an opposite bending found in the case of B2. For this system the glass transition of the polystyrene domain is at the MST¹³ and it thus prevents the formation of long-range order.

The regime of weak temperature dependence in the long-time diffusion of B1 extends from its MST to the glass transition of the polystyrene domains (≈ 320 K). The self-diffusion of the diblock copolymer in this temperature range is not controlled by free volume but by the transport across domain boundaries.

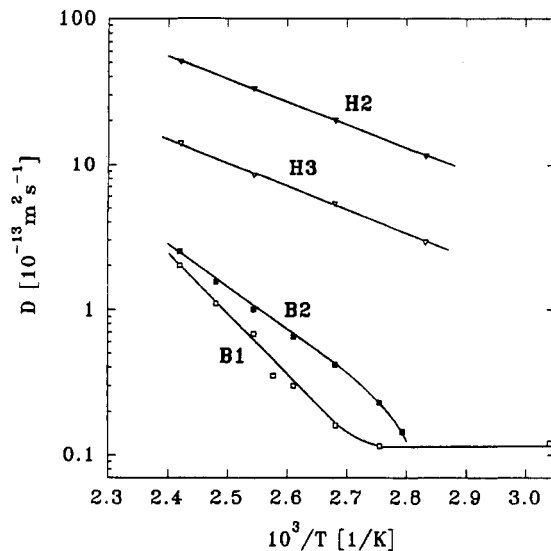


Figure 8. Temperature dependence of the diffusion coefficients of the homopolymers and the long-time diffusion coefficients (D_{slow}) of the block copolymers obtained in pulsed field gradient measurements.

V. Conclusions

Symmetric diblock copolymers of polystyrene and polyisoprene are known to exhibit concentration fluctuations even above the MST. We have shown that this regime is characterized by local ordering which is also effective as a spatial restriction on the self-diffusion of the molecules. Their diffusion is anisotropic along the lamellae.¹ Using field gradient NMR the confinement of the molecule in a cage of radius 70 nm could be shown. We suggest that the limits of this cage are domain boundaries between bundles of lamellae.

Transport across the limits of the cage happens on a longer time scale. The increase of order when traversing the MST is seen as a further slowing down of this process. The cage does not significantly grow in size, but its walls become more effective. The perfection of structure is mainly a purification of the polystyrene and polyisoprene domains, respectively.

References and Notes

- (1) Ehlich, D.; Takenaka, M.; Okamoto, S.; Hashimoto, T. *Macromolecules* **1993**, *26*, 492–498.
- (2) Stühn, B.; Rennie, A. R. *Macromolecules* **1989**, *22*, 2460.
- (3) Kärger, J.; Pfeifer, H.; Heink, W. *Adv. Magn. Reson.* **1988**, *12*, 1–89.
- (4) Bee, M. *Quasielastic neutron scattering*; Adam Hilger: Bristol, U.K., 1988.
- (5) Springer, T. *Quasielastic neutron scattering for the investigation of diffusive motions in solids and liquids. Springer tracts in modern physics*; Springer: Berlin, Heidelberg, New York, 1972; Vol. 64.
- (6) Fajara, F.; Geil, B.; Sillescu, H.; Fleischer, G. *Z. Phys. B* **1992**, *88*, 195–204.
- (7) Mori, K.; Tanaka, H.; Hasegawa, H.; Hashimoto, T. *Polymer* **1989**, *30*, 1389–1397.
- (8) Owens, J.; Gancarz, I.; Koberstein, J.; Russell, T. *Macromolecules* **1989**, *22*, 3380–3387.
- (9) Holzer, B.; Lehmann, A.; Stühn, B.; Kowalski, M. *Polymer* **1991**, *32*, 1935.
- (10) Leibler, L. *Macromolecules* **1980**, *13*, 1602–1617.
- (11) Fredrickson, G.; Helfand, E. *J. Chem. Phys.* **1987**, *87*, 697–705.
- (12) Stühn, B.; Mutter, R.; Albrecht, T. *Europhys. Lett.* **1992**, *18*, 427–432.
- (13) Stühn, B. *J. Polym. Sci., Polym. Phys.* **1992**, *30*, 1013–1019.
- (14) van Meerwall, E.; Grigsby, J.; Tomich, D.; van Antwerp, R. *J. Polym. Sci., Polym. Phys. Ed.* **1982**, *20*, 1037.
- (15) Stühn, B.; Stickel, F. *Macromolecules* **1992**, *25*, 5306–5312.
- (16) Dianoux, A. J.; Pineri, M.; Volino, F. *Mol. Phys.* **1982**, *46*, 1129–1137.
- (17) Fleischer, G.; Geschke, D.; Kärger, J.; Heink, W. *J. Magn. Reson.* **1985**, *65*, 429.